



The University of Bradford Institutional Repository

<http://bradscholars.brad.ac.uk>

This work is made available online in accordance with publisher policies. Please refer to the repository record for this item and our Policy Document available from the repository home page for further information.

To see the final version of this work please visit the publisher's website. Access to the published online version may require a subscription.

Link to publisher's version: <http://dx.doi.org/10.1039/C7EW00455A>

Citation: Al-Obaidi M, Kara-Zaitri C and Mujtaba I (2018) Significant energy savings by optimising membrane design in multi-stage reverse osmosis wastewater treatment process. *Environmental Science: Water Research & Technology*. 4(3): 449-460.

Copyright statement: © 2018 The Royal Society of Chemistry. Reproduced in accordance with the publisher's self-archiving policy.

1 **Significant energy savings by optimising membrane design in multi-stage reverse osmosis**
2 **wastewater treatment process**

3 **M. A. Al-Obaidi ^{1,2}, C. Kara-Zaitri ¹ and I. M. Mujtaba ^{1,*}**

4 ¹ Chemical Engineering, School of Engineering, Faculty of Engineering and Informatics
5 University of Bradford. Bradford, West Yorkshire BD7 1DP, UK

6 ² Middle Technical University, Iraq – Baghdad

7 *Corresponding author, Tel.: +44 0 1274 233645

8 E-mail address: I.M.Mujtaba@bradford.ac.uk

9
10 **Abstract**

11 The total energy consumption of many Reverse Osmosis (RO) plants has continuously improved
12 as a result of manufacturing highly impermeable membranes in addition to implementing energy
13 recovery devices. The total energy consumption of the RO process contributes significantly to
14 the total cost of water treatment. Therefore, any way of keeping the energy consumption to a
15 minimum is highly desirable but continues to be a real challenge in practice. Potential areas to
16 explore for achieving this include the possibility of optimising the module design parameters
17 and/or the associated operating parameters. This research focuses on this precise aim by
18 evaluating the impact of the design characteristics of membrane length, width, and feed channel
19 height on the total energy consumption for two selected pilot-plant RO process configurations
20 for the removal of chlorophenol from wastewater. The proposed two configurations, with and
21 without an energy recovery device (ERD), consist of four cylindrical pressure vessels connected
22 in series and stuffed with spiral wound membranes. A detailed steady-state model developed
23 earlier by the authors is used here to study such impact via repetitive simulation. The results
24 achieved confirm that the overall energy consumption can be reduced by actually increasing the
25 membrane width with a simultaneous reduction of membrane length at constant membrane area
26 and module volume. Energy savings of more than 60 % and 54 % have been achieved for the
27 two configurations with and without ERD respectively using process optimization. The energy
28 savings are significantly higher compared to other available similar studies from the literature.

29
30 **Keywords:** Reverse Osmosis (RO); Spiral-wound Module; Chlorophenol Removal; Energy
31 Consumption.

34 1. Introduction

35 Chlorophenol and phenolic compounds (aromatic compounds) are considered as one of the
36 common pollutants that can be found in effluents of several industrial processes such as,
37 refineries, fertilizers, petrochemical, pharmaceutical and lubricant production, which are reported
38 as having high toxicity even at low concentrations.¹ Most importantly, the existence of a small
39 trace amount of such high-toxic compounds in industrial effluents can prohibit the reuse of water
40 in many applications. High-pressure driven membrane technology is widely used for making
41 high quality water from seawater and wastewater. Interestingly, it appears that the extent of
42 energy consumption of the RO process has been steadily improved due to the development of
43 high permeability membranes in addition to incorporating the energy recovery devices.² Most
44 specifically, the total energy consumption used to drive the high-pressure pumps is considered as
45 the main constitute of total cost of water desalination.³ Significant research from academic and
46 industrial societies are made towards the reduction of energy consumption of the RO process by
47 optimising the operating conditions, investigating the number of stages, modules configuration,
48 implementing an energy recovery device (ERD) and membrane type.⁴⁻⁷ However, there are
49 some examples in the literature that highlighted the membrane characteristics optimisation and
50 its effect on the total energy consumption of an individual module of the RO process as follows:
51 [Sablani et al.](#)⁸ analysed the influence of spacer thickness of the spiral wound membrane module
52 on the permeate flux of the RO seawater desalination process. They found that there is a specific
53 intermediate spacer thickness, which yields the highest economic performance compared to other
54 feed spacers tested. [Karabelas et al.](#)⁹ studied the optimisation of a spiral-wound RO seawater
55 and brackish desalination system operation by measuring the sensitivity of varying the element
56 design variables, including feed and permeate spacer characteristics (channel gap) and sheet
57 width (at a constant total area), on the operating variables including permeate flux, trans-
58 membrane pressure, retentate and permeate pressures, and feed velocity. Their optimisation
59 results showed that the permeate-side variation affected the trans-membrane pressure and
60 module productivity directly. It was also found that the retentate-side spacer could be used to
61 control the pressure drop across the element, and that the overall performances of low and high-
62 pressure membranes are increased when using short sheets of membrane. [Sharifanfar et al.](#)¹⁰
63 affirmed that the recovery rate of the pomegranate juice clarification process is significantly
64 affected by the size of the feed canal height of microfiltration membrane. [Gu et al.](#)¹¹ investigated

65 the impact of the height of both feed and permeate channels, membrane dimensions and centre
66 pipe radii, on the performance and energy consumption of a spiral-wound RO desalination
67 process. While [Al-Obaidi et al.](#)¹² optimised the energy consumption of an individual spiral-
68 wound RO module for the removal of dimethylphenol from wastewater. They achieved this by
69 manipulating the module dimensions including membrane length, width, and feed channel
70 height. The net outcome of this is that the energy consumption has been reduced by 19.2 % in
71 comparison with the standard module measurements. To the best of authors' knowledge, the
72 impact of membrane design characteristics of multi-stage RO wastewater process on energy
73 consumption has not yet been explored fully and therefore requires further research. The aim of
74 this paper is to attempt this challenge by studying several repetitive optimisation scenarios to
75 examine the impact of varying the membrane and module specifications on the overall energy
76 consumption and recovery rate of a multi-stage RO process for the removal of chlorophenol from
77 wastewater. This will be carried out by studying the consequences of altering the membrane
78 dimensions (length and width) at constant area, and feed channel height at a varied module
79 volume, as well as increasing the membrane area outside the manufacturer's specification. A
80 further investigation is carried out to specifically explore the outcomes of two proposed
81 configurations of membrane design with and without ERD on the total energy saving. The
82 starting point of this research is to explore if even more potential energy can actually be saved by
83 optimising the membrane dimensions of multi-stage RO process beyond what has already been
84 achieved by [Al-Obaidi et al.](#)¹² in an individual RO module but this time for the removal of
85 chlorophenol.

86 The model of [Al-Obaidi et al.](#)¹², which included the thermodynamic and mass transfer properties
87 of chlorophenol, can readily be adapted for use in this research. The model has already been
88 validated against experimental data obtained for the removal of dimethylphenol in an individual
89 membrane pilot-plant. The detail of this model and the thermophysical properties of
90 chlorophenol are given in [Tables A.1 and A.2](#) in [Appendix A](#) for convenience. Moreover, the
91 model has been validated taking into consideration the experimental results of [Sundaramoorthy](#)
92 [et al.](#)¹³ for the removal of chlorophenol from wastewater using an individual RO membrane
93 module. The validation results of this study are given in [Table A.3](#) in [Appendix A](#), which show a
94 good match between the model prediction and the experimental data. Finally, the model is
95 further tailored by including [Eqs. \(17\) and \(18\)](#) ([shown in Table A.1 in Appendix A](#)) to consider

96 the calculation of the energy consumption for each proposed configuration (A and B) of the
97 multi-stage RO process shown in Fig. 1.

98

99

100

101

102

Fig. 1. Schematic diagram of two tapered configurations A and B of the RO pilot-scale plant.

103

104

2. Plant description and feed characteristics

105

106

107

108

109

110

111

112

113

114

115

116

117

118

119

120

121

122

123

124

125

126

This section describes the characteristics of the two proposed configurations of the multi-stage RO wastewater pilot-plant. Fig. 1 shows the schematic diagrams of configurations A and B, each containing four series pressure vessels (three stages) stuffed with spiral wound modules using the membrane type Ion exchange, India of 7.845 m². Stage 1 contains two parallel modules while one module designed for stages 2 and 3. The design of retentate reprocessing is used where the permeate of three pressure vessels is blended to form the product stream. The technical details of the membrane used in the two configurations are identical to those used by Sundaramoorthy *et al.*¹³, where a single element is used to remove chlorophenol from wastewater, as shown in Table 1. Configurations A and B are similar except that B has an energy recovery device (ERD) and booster pump (BP), both used to reduce the overall energy consumption. Moreover, the feed stream is split into two parts. The first part is directly pumped using a high-pressure pump (efficiency 85 %), which can deliver a maximum operating pressure of 20 atm. The second part is fed back to the ERD (efficiency 80 %) to raise its pressure using a high-pressure retentate stream. More specifically, ERD is used to transfer the energy from the high-pressure retentate stream to the low-pressure feed stream, using a rotary turbine that initiates a secondary pump to pressurize the feed. For operational safety reasons, the inlet streams of ERD of low-pressure feed and high-pressure retentate should be equal. Most importantly, it is necessary to use a booster pump, which can raise the feed stream to the required operating pressure. The design of configuration B shown in Fig. 1 is identical to the one by Oh *et al.*¹⁴ in seawater desalination RO process. Finally, the transport parameters of water and chlorophenol and the membrane friction parameter are derived from Sundaramoorthy *et al.*¹³ and given in Table 2.

127 **Table 1.** Membrane characteristics and geometry of Ion Exchange, India Ltd.*

128

129 **Table 2.** Transport parameters and membrane friction factor

130

131 **3. Simulation of the RO process**

132 In this section, the RO process of the two configurations A and B with and without ERD (Fig. 1)
133 is simulated using four sets of operating conditions of feed concentration, flow rate, pressure,
134 and temperature as follows:

135 1. 6.226E-3 kmol/m³, 4.66E-4 m³/s, 11 atm, 29 °C.

136 2. 6.226E-3 kmol/m³, 4.66E-4 m³/s, 15 atm, 31 °C.

137 3. 6.226E-3 kmol/m³, 5.166E-4 m³/s, 13.58 atm, 30 °C.

138 4. 6.226E-3 kmol/m³, 5.166E-4 m³/s, 15 atm, 33 °C.

139 Please note that the selected sets of operating conditions are within the operating conditions of
140 [Sundaramoorthy et al.](#)¹³ except for the feed flow rate where it is chosen to fulfil the
141 requirements of two parallel modules in the first stage (Fig. 1).

142 **Table 3** shows simulation results of the two configurations considering the total energy
143 consumption, chlorophenol removal, and total water recovery. Moreover, these results are
144 compared to the maximum chlorophenol rejection rate of [Sundaramoorthy et al.](#)¹³ of an
145 individual RO module (Ion Exchange, India) used to remove chlorophenol from wastewater. It is
146 important to note that the maximum performance achieved by [Sundaramoorthy et al.](#)'s¹³
147 experiment is conducted at operating conditions of 6.226E-3 kmol/m³, 2.583E-4 m³/s, 13.58 atm
148 and 31 °C of inlet chlorophenol concentration, feed flow rate, pressure, and temperature
149 respectively. The results achieved in configurations A and B clearly show that the total recovery
150 rate is higher than that obtained from the individual RO module. It can therefore be concluded
151 that the proposed fixed-size configurations with and without ERD yield more energy saving than
152 the single-stage RO process ([Sundaramoorthy et al.](#)¹³) with the same membrane specifications.
153 Having said, it is acknowledged that this improvement comes with the penalty of a greater
154 membrane cost. Incidentally, [Zhu et al.](#)⁶ confirm the same findings for the RO desalination
155 process. While [Li](#)⁷ found that more energy can be saved when increasing the number of stages
156 (no more than five) and using an ERD. It would therefore be interesting to evaluate the impact of
157 module dimensions on the performance of these configurations.

158
159
160
161
162
163
164
165
166
167
168
169
170
171
172
173
174
175
176
177
178
179
180
181
182
183
184
185
186
187
188
189

Table 3. Simulation results

4. Impact of design parameters

This part of the research discusses the impact of varying the membrane and module specifications (outside the manufacturer’s specifications presented in [Table 1](#)) for a given set of operating conditions on the energy consumption, total water recovery, and chlorophenol rejection for the two configurations A and B of [Fig. 1](#). Most importantly, the modification of membrane and module specification is carried out simultaneously for all the modules shown in [Fig. 1](#).

4.1 Effects of altering membrane width and length concurrently at constant area and module volume

The membrane dimensions (width and length) of each module for configurations A and B are simultaneously changed when both the volume and membrane area are kept constant, as per the original manufacturer’s specification. The initial expectation is that this change will amend the flow patterns associated with the feed fluid within the membrane module.

The geometry optimisation of the membrane type Ion Exchange - India is carried out in the simulated operating conditions of $5.166E-4$ m³/s, 15 atm and 31 °C and initial chlorophenol concentration of $6.226E-3$ kmol/m³. The effect of 5 % step change reductions in membrane length (increase the width) at constant area of 7.845 m² and module volume (height of the feed channel of 0.8E-3 m) for all the modules of configurations A and B on chlorophenol rejection and total recovery rate is given in [Fig. 2](#). While [Fig. 3](#) shows the impact of membrane width increase at constant membrane area and volume on the energy consumption of configurations A and B.

Fig. 2. Effect of 5 % step change reduction in membranes length at constant membrane area on chlorophenol rejection and water recovery (inlet feed conditions, $6.226E-3$ kmol/m³, $5.166E-4$ m³/s, 15 atm and 31 °C)

190

191

192 **Fig. 3.** Effect of 5 % step change reduction in membranes length at constant membrane area on specific energy
193 consumption of configurations A and B (inlet feed conditions, $6.226\text{E-}3$ kmol/m³, $5.166\text{E-}4$ m³/s, 15 atm and 31 °C)

194

195 It is not difficult to see that the rejection parameter is gradually decreased due to an increase in
196 membrane width at constant membrane area (Fig. 2). However, an increase in total water
197 recovery is observed as a result of this variation. It is alleged that the reason for this phenomenon
198 is that the reduction of the membrane length results in a decrease of the loss of the operating
199 pressure along the membrane length, which in turn promotes the flux of water and increases the
200 total recovery. Lomax ¹⁵ confirmed that shorter sheets with many envelopes (longer width) for a
201 given total membrane area have a clear permeate flux and total recovery advantage. Also,
202 Karabelas *et al.* ⁹ showed that increasing the membrane width at a constant membrane area
203 improved the performance of seawater RO membrane with a constraint of module diameter that
204 can hold a maximum number of membrane envelopes.

205 Fig. 3 also shows that the reduction of the membrane length yields a reduction in the
206 consumption of energy in both the configurations tested, albeit with an even better result in pilot-
207 plant B. Reducing the membrane length has yielded a maximum reduction of chlorophenol
208 rejection to about 5.18 % with a 5.26 % increase in recovery rate with around 13 % and 5 %
209 energy consumption reduction with and without ERD respectively. These results confirm the
210 advantages of configuration B in energy consumption despite a small decrease in chlorophenol
211 rejection percentage.

212

213 **4.2 Effect of altering the feed channel height at constant area and variable module volume**

214 This section explores the effect of feed channel height on the RO process, since the feed spacers
215 readily come in different thicknesses and geometries. The feed spacers, in turn, influence the rate
216 of turbulence and the fluid flow hydrodynamics. The influence of increasing feed channel height
217 on chlorophenol rejection and total recovery rate is shown graphically in Fig. 4. This readily
218 shows that the feed channel height increases outside the manufacturer's specification despite
219 keeping a constant membrane area but with a variable module volume for all the modules
220 connected as shown in configuration A and B (Fig. 1) at constant operating feed conditions. Fig.

221 5 shows a similar impact of the feed channel height on the energy consumption of configurations
222 A and B.

223

224

225 **Fig. 4.** Effect of feed channel height on chlorophenol rejection and total recovery (inlet feed conditions, $6.226\text{E-}3$
226 kmol/m^3 , $5.166\text{E-}4 \text{ m}^3/\text{s}$, 15 atm and $31 \text{ }^\circ\text{C}$)

227

228

229

230 **Fig. 5.** Effect of feed channel height on energy consumption of configurations with and without ERD (inlet feed
231 conditions, $6.226\text{E-}3 \text{ kmol/m}^3$, $5.166\text{E-}4 \text{ m}^3/\text{s}$, 15 atm and $31 \text{ }^\circ\text{C}$)

232

233 Interestingly, **Fig. 4** shows that chlorophenol rejection and total recovery rate are decreasing as
234 the feed channel height increases. This in turn retards the energy consumption of both
235 configurations tested (**Fig. 5**). This is due to an increase in pressure drop caused by increasing the
236 height of the feed channel in addition to a clear reduction in feed velocity caused by increasing
237 the module volume. This causes a reduction in the driving force of water flux and ultimately
238 reduces the rejection parameter. Furthermore, increasing the feed channel height has a significant
239 negative impact on the total recovery in comparison to altering the dimensions of membranes
240 width and length as can be seen in **Fig. 2**, which improves the total recovery rate. Therefore,
241 increasing the feed channel height from $0.5\text{E-}3$ to $1\text{E-}3 \text{ m}$ causes 25.31 % and 30.39 % reduction
242 in rejection parameter and recovery rate respectively, while an increase of the energy
243 consumption of 37.24 % and 43.26 % occurs for configurations with and without ERD
244 respectively.

245

246 **4.3 Effect of increasing the membrane area by an incremental increase of membrane** 247 **dimensions**

248 This section explores the effect of increasing the membrane area by 50 % of all the modules of
249 configurations A and B (shown in **Fig. 1**), starting from the original membrane value of 7.845 m^2
250 and increasing it incrementally to 11.768 m^2 . This is implemented using the following two
251 options:

- 252 1) A 50 % increase in membrane length of 10 % step change with keeping a constant
253 membrane width of 8.4 m and feed channel height of $0.8\text{E-}3 \text{ m}$.

254 2) A 50 % increase in membrane width of 10 % step change with keeping a constant
255 membrane length of 0.934 m and feed channel height of 0.8E-3 m at constant operating
256 feed conditions on chlorophenol rejection, total recovery rate, and energy consumption of
257 configurations A and B is shown in Figs. 6 and 7.

258
259 Fig. 6 readily shows that the chlorophenol rejection is kept more or less constant, where it
260 decreases from 81.92 % to 79.34 % at 0.3 % reduction when the membrane area increases as a
261 result of an increase in the membrane length from 0.934 m to 1.4 m. However, a 50 % increase
262 in the membrane, applied by increasing the membrane width from 8.4 to 12.6 m, causes a
263 reduction of about 6.58 % in chlorophenol rejection from 81.92 % to 76.53 %.

264 Fig. 6 shows that an increase in the membrane area from 7.845 m² to 11.768 m² causes a
265 considerable increase of 30.90 % from 48.11 % to 62.98 % and 39.76 % from 48.11 % to 67.25
266 % in total recovery rate as a response to an increase in the membrane width and length
267 respectively. As expected, Fig. 7 shows that an increase in the membrane area in both the options
268 tested causes a reduction in energy consumption. Therefore, the energy consumption of
269 configuration A without ERD decreases by 23.6 % from 1.03 kWh/m³ to 0.78 kWh/m³ and 28.44
270 % from 1.03 kWh/m³ to 0.73 kWh/m³ when increasing the membrane area; i.e. by increasing the
271 membrane width and length respectively. On the other hand, the energy consumption of
272 configuration B with ERD decreases by 15.81 % from 0.83 kWh/m³ to 0.70 kWh/m³ and 24.08
273 % from 0.83 kWh/m³ to 0.63 % when increasing the membrane area; i.e. by increasing the
274 membrane width and length respectively. It can therefore be concluded that a 50 % increase of
275 membrane area due to an increase in the membrane width at constant length is preferable
276 because it has a positive impact on the total recovery rate and energy consumption of the
277 configurations tested (especially B) albeit with a small reduction in chlorophenol rejection of
278 6.58 %. This is compared to the consequence of increasing the membrane area by increasing the
279 membrane length but with a constant width. The clear feed velocity reduction in all modules is
280 essentially the main reason for 6.58 % reduction in the chlorophenol rejection mainly due to an
281 increase in the membrane width at a constant length. The next step is therefore to investigate
282 reductions of 37.66 %, 46.89 % and 50.05 % in feed velocity of stages 1, 2 and 3 respectively
283 after the 50 % increase in the membrane width at constant length. These will be compared to
284 similar reductions of 6.62 %, 19.47 and 26.04 % due to 50 % increase in the membrane length at

285 constant width. The rationale here is that this process increases the accumulated chlorophenol at
286 the membrane wall and it therefore increases the permeate concentration as a result of an
287 increase of the solute flux through the membrane.

288

289

290 **Fig. 6.** Effect of 50 % membrane increase caused by separate membranes length and width increasing on
291 chlorophenol rejection and total recovery rate (initial conditions, $6.226\text{E-}3$ kmol/m³, $5.166\text{E-}4$ m³/s, 15 atm and 31
292 °C)

293

294

295 **Fig. 7.** Effect of 50 % membrane increase caused by separate membranes length and width increasing on energy
296 consumption of configurations of with and without ERD (initial conditions, $6.226\text{E-}3$ kmol/m³, $5.166\text{E-}4$ m³/s, 15
297 atm and 31 °C)

298

299 **Fig. 8** shows the progress of permeate concentration for the two scenarios of increasing the
300 membrane area due to an increase in the membrane length and width respectively. It can readily
301 be seen that an increase in the membrane area due to an increase in the membrane width has a
302 higher passive impact on the permeate concentration of all the stages. Moreover, the gain of total
303 water recovery after increasing the membrane width at constant length is higher than what can be
304 achieved after increasing the membrane length in constant width. This is because of higher
305 pressure loss occurs in all the modules as a result of an increase in the membrane length at a
306 constant width compared to the second scenario. This causes a reduction of the quantity of water,
307 which penetrates the membrane compared to the original membrane length. Simulation results
308 for this scenario show a total reduction of 20.47 % occurring in the outlet plant pressure after a
309 50 % increase in the membrane length of each module, compared to 17.45 % reduction after a 50
310 % increase in the membrane width. It can therefore be concluded that more reduction of energy
311 consumption in the two configurations with and without ERD can be achieved by increasing the
312 membrane area based on an increase in the membrane width at constant length (**Fig. 7**).

313

314

315

316

317 **Fig. 8.** Effect of 50 % membrane increase caused by separate membranes length and width increasing on
318 chlorophenol permeate concentrations at the three stages rejection (initial conditions, $6.226\text{E-}3$ kmol/m³, $5.166\text{E-}4$
319 m³/s, 15 atm and 31 °C)

320

321 **4.4 Effect of increasing the membrane area by a synchronous increase of membrane length** 322 **and width**

323 This section explores the influence of increasing the membrane area on the performance of a
324 multi-stage RO process for removing chlorophenol from wastewater. More specifically, the area
325 is increased by 50 % by synchronously increasing the membrane length and width of all the
326 modules at the constant original manufacture's feed channel height of $0.8\text{E-}3$ m.

327 The simulation results shown in [Fig. 9](#) confirm 4.82 % reduction in chlorophenol rejection but
328 36.42 % increase of total water recovery as a result of increasing the membrane area by 50 %.

329 The simulation results shown in [Fig. 10](#) show 20.97 % and 26.69 % reduction of total energy
330 consumption for configurations A and B; i.e. with and without ERD respectively. It can therefore
331 be concluded that an increase of the membrane area yields less energy consumption but also
332 reduced chlorophenol rejection. It can be concluded furthermore that increasing the membrane
333 area by 50 % by increasing the membrane width at constant length and feed channel height
334 yields higher reduction of energy consumption in comparison to increasing the membrane length
335 and synchronously increasing membrane length and width in both configurations.

336

337

338 **Fig. 9.** The effect of 50 % membrane increase caused by the synchronous membranes length and width increasing
339 on chlorophenol rejection and total recovery rate (initial conditions, $6.226\text{E-}3$ kmol/m³, $5.166\text{E-}4$ m³/s, 15 atm and
340 31 °C)

341

342

343

344

345 **Fig. 10.** The effect of 50 % membrane increase caused by the synchronous membranes length and width increasing
346 on energy consumption of configurations of with and without ERD (initial conditions, $6.226\text{E-}3$ kmol/m³, $5.166\text{E-}4$
347 m³/s, 15 atm and 31 °C)

348

349 Clearly the interplay between the total energy consumption and the chlorophenol rejection will
350 need further investigation. This is the subject of the next section, which discusses a multi-
351 objective optimisation study using the gPROMS software.¹⁶ This study concurrently explores the
352 impact of all the membrane dimensions while maximising the reduction of energy consumption
353 and chlorophenol rejection for the two proposed configurations, with and without ERD.

354

355 **5. Optimisation results of the two RO process configurations with and without ERD**

356 This is carried out using the gPROMS optimisation tool, where the minimisation of the energy
357 consumption and maximization of the chlorophenol rejection are considered to be the objective
358 functions at the selected operating conditions of 6.226E-3 kmol/m³, 5.166E-4 m³/s, 15 atm and
359 31 °C of feed chlorophenol concentration, feed flow rate, pressure, and temperature respectively.
360 The module dimensions of all the membranes including; length, width, and feed channel height
361 are considered as the design parameters selected within upper and lower limits shown in [Table 4](#).
362 Since the membrane type used in this simulation is Ion Exchange, India, the value of the area of
363 7.845 m² is set as a constraint.

364 The non-linear algebraic model equations shown in [Table A.1](#) of [Appendix A](#) are written in the
365 following compact form:

366 $f(x, u, v) = 0$, where:

- 367 • x is the set of all algebraic variables,
- 368 • u is the set of decision variables (to be optimised), and
- 369 • v denotes the constant parameters of the process.

370 The function f is assumed to be continuously differentiable with respect to all their arguments.

371

372 **Table 4.** Limits of optimisation operational parameters

373

374

375 The optimisation problem will be mathematically written as follows:

- 376 • Given: Operating feed parameters, module specifications.
- 377 • Optimise: Membrane dimensions.
- 378 • Minimise: The total energy consumption.

- 379 • Maximise: The chlorophenol rejection.
- 380 • Subject to: Equality (process model) and inequality constraints (linear bounds of
- 381 optimisation variables

382 There are therefore two optimisation problems, as represented mathematically below:

$$\begin{array}{ll}
 383 & \text{Min} & T.E.C.1 \quad \text{and} \quad T.E.C.2 \\
 384 & \text{Max} & Rej_{(Total)} \\
 & L, W, t_f &
 \end{array}$$

385
386 Subject to:

387 Equality constraints:

388 Process Model: $f(x, u, v) = 0$

389 Inequality constraints:

$$\begin{array}{l}
 390 \quad L^L \leq L \leq L^U \\
 391 \quad W^L \leq W \leq W^U \\
 392 \quad t_f^L \leq t_f \leq t_f^U
 \end{array}$$

393 End-point constrain: $A = 7.845 \text{ m}^2$

394
395 **6. Optimisation results**

396 The optimisation results of the multi-stage RO process are given in [Table 5](#), which shows the
 397 optimum values of membrane length (L), width (W), and feed channel height (t_f) for each stage
 398 and the optimised total energy consumptions of configurations A ($T.E.C.1$) and B ($T.E.C.2$) at
 399 the maximum chlorophenol rejection $Rej_{(Total)}$ and recovery rate $Rec_{(Total)}$ achieved. It is
 400 noteworthy to mention that the optimisation platform of gPROMS has given only one solution,
 401 instead of a set of non-dominant solutions as the case of Genetic Algorithm.¹⁷

402
403
404
405 **Table 5.** Optimal optimisation results of multi-stage RO process of with and without ERD at operating conditions of
 406 (initial conditions, 6.226E-3 kmol/m³, 5.166E-4 m³/s, 15 atm and 31 °C)

407

408 Firstly, it can be said that the total energy consumption can be reduced further when discarding
409 the second objective function relating to maximising the chlorophenol rejection. However, the
410 optimal results shown in [Table 5](#) point to the possibility of having a higher rejection parameter at
411 a lower energy consumption. In order to keep the highest water flux, the results also confirm the
412 necessity to select specific membrane dimensions for stage 2 compared to similar specifications
413 for stages 1 and 3. In other words, the alteration of stage 2 module dimensions was necessary for
414 maximising the total recovery rate of this stage. This is the result of blending the two high
415 concentration streams of stage 1, which induces the high feed flow rate stream of stage 2 (one
416 pressure vessel). Therefore, the increase of the membrane width and the decrease of the
417 membrane length play a significant role in reducing the feed flow rate along the whole section
418 and yield a higher water flux and sustainable energy saving. Most importantly, the total energy
419 consumption of configurations A and B exhibit a significant reduction of energy consumption -
420 about 60.32 % from 2.034 kWh/m³ to 0.807 kWh/m³ and 54.42 % from 2.034 kWh/m³ to 0.927
421 kWh/m³ for configurations A and B respectively compared with the maximum performance of
422 the individual membrane pilot-scale experiment of [Sundaramoorthy *et al.*¹³](#). Essentially, the total
423 recovery rate achieved in the proposed configurations is 53.55 % compared to only 22 % as per
424 [Sundaramoorthy's *et al.*¹³](#) experiment. For convenience, the operating conditions at the
425 maximum performance of [Sundaramoorthy's *et al.*¹³](#) experiment are given in [Section 3](#). Having
426 said the above, the total chlorophenol rejection achieved represents an increase of 12.6 % (from
427 83 % to 93.5 %) compared to the maximum rejection reported in the experiment of
428 [Sundaramoorthy *et al.*¹³](#). In the majority of cases, the capacity of the proposed configurations is
429 comparable with the study of [Al-Obaidi *et al.*¹²](#), who achieved a maximum reduction of 19.2 %
430 in total energy consumption of an individual spiral-wound RO module used to remove
431 dimethylphenol from wastewater.

432 [Table 5](#) shows that the optimum value of feed channel height is 0.5E-3 m. This is deemed
433 reasonable in the case of removing chlorophenol because of the low possibility of fouling or
434 scaling in the presence of low feed concentration (6.226-3 kmol/m³ equivalent to 800 ppm). This
435 implies that a higher feed channel height value would be required in the optimisation problem
436 when treating higher feed chlorophenol concentrations.

437 The results of this research have confirmed that the RO process can readily be used to achieve
438 the stringent limits of high-toxic compounds concentration, which are set to increase in the

439 future. The methodology presented in this research can also be easily implemented for complex
440 wastewater of organic and non-organic compounds. However, the contribution of all compounds
441 to the osmotic pressure must be assessed, and the extent to which the RO process presented in
442 Fig. 1 can be successfully used to abate a complex wastewater must be explored. This is because
443 chlorophenol has high hydrophilicity properties in water (easily dissolved in water).¹⁸ Therefore,
444 such complex wastewater rejection and energy consumption aspects of a multi-stage RO process
445 need to be investigated in the future.

446

447 **7. Conclusions**

448 The impact of varying the membrane and module specifications on the overall energy
449 consumption, chlorophenol rejection and total recovery rate has been investigated using two
450 configurations of multi-stage RO process, with and without ERD for the removal of
451 chlorophenol from wastewater.

452 Specifically, the research confirms the following key conclusions:

- 453 1. In a conventional RO plant, increasing the membrane width and decreasing the
454 membrane length outside the manufacturer's specification and at the same time keeping a
455 constant membrane area and module volume, yields a decrease in energy consumption
456 but with a relatively small negative impact on chlorophenol rejection.
- 457 2. A noticeable increase of chlorophenol rejection, recovery rate, and decrease of energy
458 consumption can be achieved by using a low feed channel height within a constant
459 membrane area
- 460 3. A 50 % increase in the membrane area achieved by increasing the width at constant
461 length is highly desirable as it yields a significant energy consumption reduction in the
462 configurations tested, more so in B, despite a small reduction in chlorophenol rejection.
- 463 4. A 50 % increase in the membrane area achieved by concurrently increasing length and
464 width at a constant module volume can lift the reduction of energy consumption despite
465 the low reduction in chlorophenol rejection.
- 466 5. The multi-objective optimisation study identified the best module dimensions, which
467 yield the lowest energy consumption and the highest chlorophenol rejection.
- 468 6. The multi-stage RO process can save more energy consumption in comparison to a single
469 stage RO process because of the improvement made in the total recovery rate.

470 7. At least 60 % and 54 % energy consumption savings can be achieved with
471 configurations A and B, with and without ERD, respectively in comparison with
472 published data for an individual RO module (Sundaramoorthy *et al.*,¹³).

473 The above results are encouraging in that the performance of the RO system investigated can be
474 enhanced further by implementing a high permeability membrane type, one that can save both
475 energy and money and impact more definitely on the environmental. The next step of this
476 research is to continue the investigation of both configurations with a higher chlorophenol
477 concentration feed, with the expectation of a reduced energy cost per volume of produced
478 permeate.

479

480 **Nomenclature**

481 A : Effective area of the membrane (m^2)

482 A_w : Solvent transport coefficient ($m/atm\ s$)

483 b : Feed and permeate channels friction parameter ($atm\ s/m^4$)

484 B_s : Solute transport coefficient (m/s)

485 C_b : The bulk feed solute concentrations at the feed channel ($kmol/m^3$)

486 C_f : The inlet feed solute concentrations at the feed channel ($kmol/m^3$)

487 $C_{f(plant)}$: The inlet chlorophenol concentration of the plant ($kmol/m^3$)

488 C_m : The dimensionless solute concentration in Eq. (1) in Table A.2 of Appendix A
489 (dimensionless)

490 C_p : The permeate solute concentration at the permeate channel ($kmol/m^3$)

491 C_w : The solute concentration on the membrane surface at the feed channel ($kmol/m^3$)

492 D_b : The solute diffusion coefficient of feed at the feed channel (m^2/s)

493 D_p : The solute diffusion coefficient of feed at the permeate channel (m^2/s)

494 de_b : The equivalent diameters of the feed channel (m)

495 de_p : The equivalent diameters of the permeate channel (m)

496 J_s : The solute molar flux through the membrane ($kmol/m^2\ s$)

497 J_w : The permeate flux (m/s)

498 k : The mass transfer coefficient at the feed channel (m/s)

499 L : The length of the membrane (m)

500 m_f : Parameter in Eqs. (7) and (8) in Table A.2 of Appendix A

501 $P_{f(in)}$: The inlet feed pressure (atm)

502 $P_{f(out)}$: The outlet feed pressure (atm)

503 $P_{f(plant)}$: Plant feed pressure (atm)

504 P_p : The permeate channel pressure (atm)

505 Q_b : The bulk feed flow rate at the feed channel (m³/s)

506 Q_f : The inlet feed flow rate at the feed channel (m³/s)

507 $Q_{f(plant)}$: Plant feed flow rate (m³/s)

508 Q_p : The permeate flow rate at the permeate channel (m³/s)

509 Q_r : The retentate flow rate at the feed channel (m³/s)

510 R : The gas law constant ($R = 0.082 \text{ atm m}^3/\text{K kmol}$)

511 Re_b : The Reynold number at the feed channel (dimensionless)

512 Rec : Total permeate recovery (dimensionless)

513 $Rec_{(Total)}$: Total water recovery rate of the plant (dimensionless)

514 Rej : The solute rejection coefficient (dimensionless)

515 $Rej_{(Total)}$: Total chlorophenol rejection of the plant (dimensionless)

516 Re_p : The Reynold number at the permeate channel (dimensionless)

517 T : The feed temperature (°C)

518 $T_{(plant)}$: Plant feed temperature (°C)

519 $T.E.C. 1$: Total energy consumption of the plant without ERD (kW h/m³)

520 $T.E.C. 2$: Total energy consumption of the plant with ERD (kW h/m³)

521 t_f : Height of feed channel (m)

522 t_p : Height of permeate channel (m)

523 U_b : The bulk feed velocity at the feed channel (m/s)

524 W : The membrane width (m)

525 **Subscript**

526 μ_b : The Feed viscosity at the feed channel (kg/m s)

527 μ_p : The permeate viscosity at the permeate channel (kg/m s)

528 ρ_b : The feed density at the feed channel (kg/m³)

529 ρ_p : The permeate density at the permeate channel (kg/m³)

530 ρ_w : Molal density of water (55.56 kmol/m³)

531 θ : Parameter in Eq. (11) in Table A.1 of Appendix A

532

533 **References**

534 1 A. A. Gami, M. Y. Shukor, K. Abdul Khalil, F. A. Dahalan, A. Khalid and S. A. Ahmad,
535 *Journal of Environmental Microbiology and Toxicology*, 2014, 2(1), 11-24.

536 2 C. Fritzmann, J. Löwenberg, T. Wintgens and T. Melin, *Desalination*, 2007, 216, 1-76.

537 3 T. Manth, M. Gabor and E. Oklejas, *Desalination*, 2003, 157, 9-21.

538 4 F. Maskan, D. E. Wiley, L. P. M. Johnston and D. J. Clements, *AIChE J.*, 2000, 46, 946-
539 954.

540 5 A. Villafafila and I. M. Mujtaba, *Desalination*, 2003, 155, 1-13.

541 6 A. Zhu, P. D. Christofides and Y. Cohen, *Industrial and Engineering Chemistry Research*,
542 2009, 48, 6010-6021.

543 7 M. Li, *Desalination*, 2011, 276, 128-135.

544 8 S. S. Sablani, M. F. A. Goosen, R. Al-Belushi and V. Gerardos, *Desalination*, 2002, 146,
545 225-230.

546 9 A. J. Karabelas, C. P. Koutsou, and M., Kostoglou, *Desalination*, 2014, 332, 76-90.

547 10 R. Sharifanfar, H. Mirsaeedghazi, A. Fadavi, H. M. Kianmehr, *Desalination and Water
548 Treatment*, 2014, 1-7.

549 11 B. Gu, X. T. Xu and C. S. Adjiman, *Computer and Chemical Engineering*, 2017, 96, 248-
550 265.

551 12 M. A. Al-Obaidi, C. Kara-Zaitri and I. M. Mujtaba, presented in part at Proceedings of the
552 27th European Symposium on Computer Aided Process Engineering – ESCAPE 27,
553 Barcelona, Spain, October 1st - 5th, 2017.

554 13 S. Sundaramoorthy, G. Srinivasan and D. V. R. Murthy, *Desalination*, 2011, 277 (1-3),
555 257-264.

556 14 H. Oh, T. Hwang and S. A. Lee, *Desalination*, 2009, 238, 128-139.

557 15 I. Lomax, *Desalination*, 2008, 224, 111-118.

558 16 Process System Enterprise Ltd. gPROMS Introductory User Guide. London: Process
559 System Enterprise Ltd., 2001.

560 17 M. A. Al-Obaidi, J- P. Li, C. Kara-Zaitri and I. M. Mujtaba, *Chemical Engineering*
561 *Journal*, 2017, 316, 91-100.

562 18 R. C. Hudson, Hazardous materials in the soil and atmosphere, treatment removal and
563 analysis. Nova Science Publishers, Inc., New York, 2006.

564 19 C. Koroneos, A. Dompros and G. Roumbas, *Journal of Cleaner Production*, 2007, 15,
565 449-464.

566

567

568

569

570

571

572

573

574

575

576

577

578

579

580

581

582

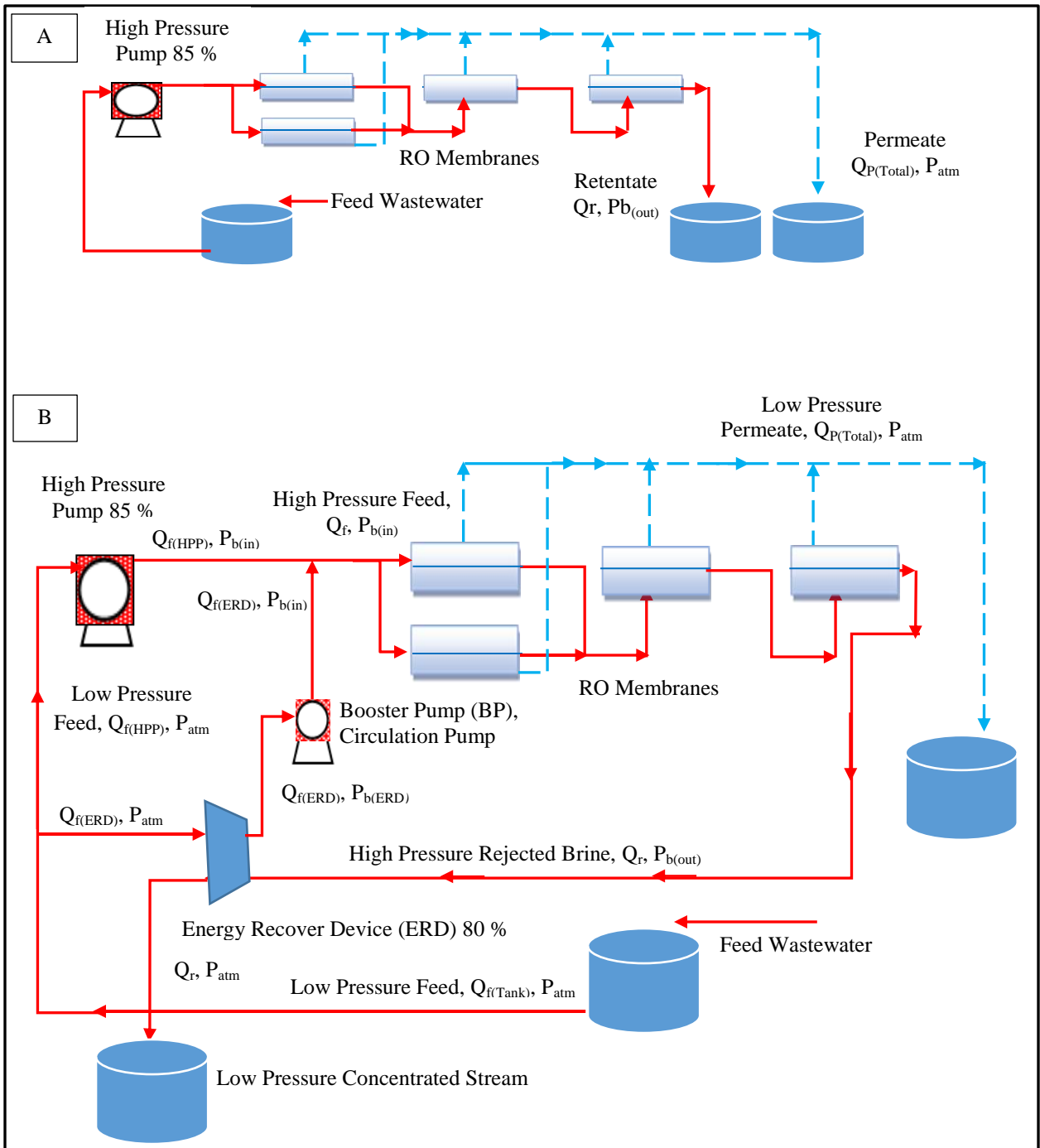
583

584

585

586

587 **Fig. 1**



588

589

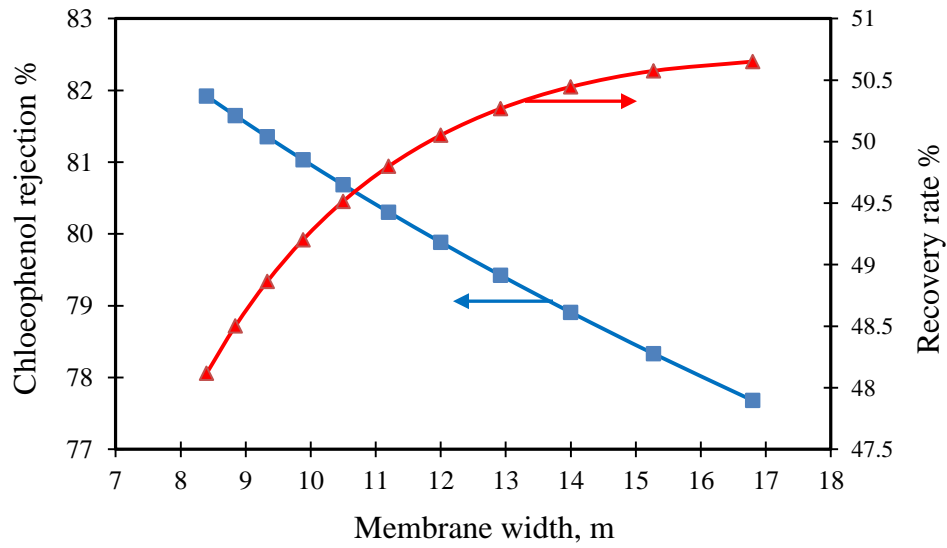
590

591

592

593

Fig. 2

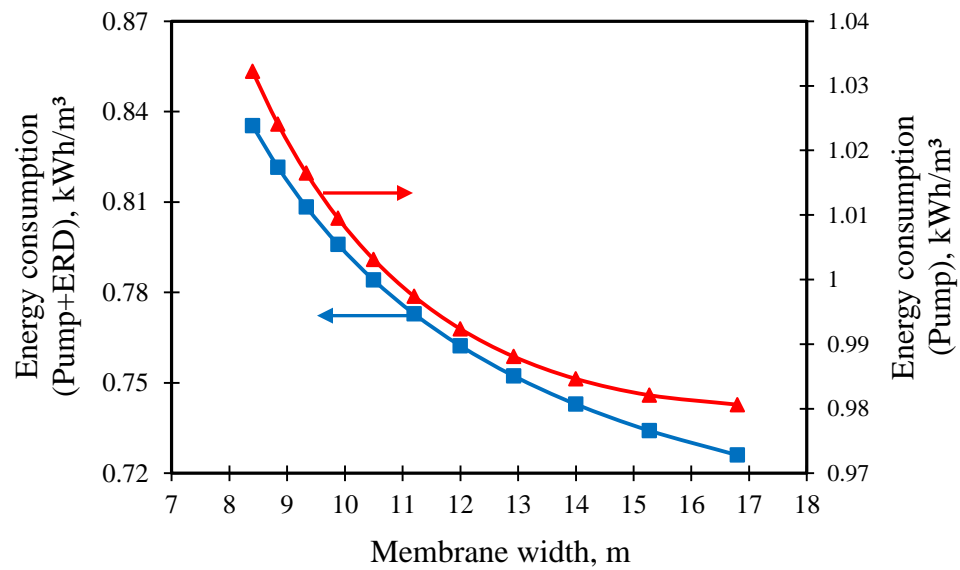


594

595

596

Fig. 3.



597

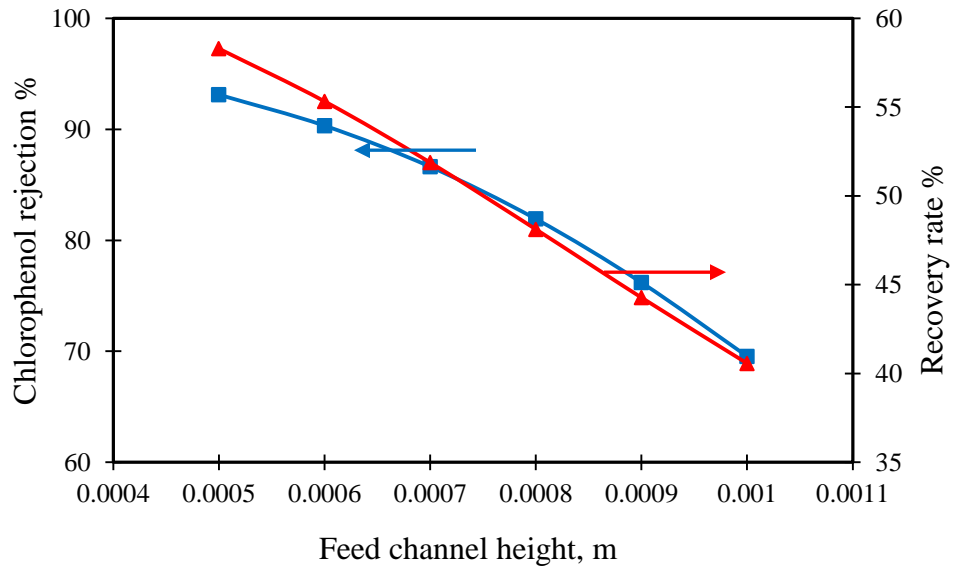
598

599

600

601

602 **Fig. 4.**

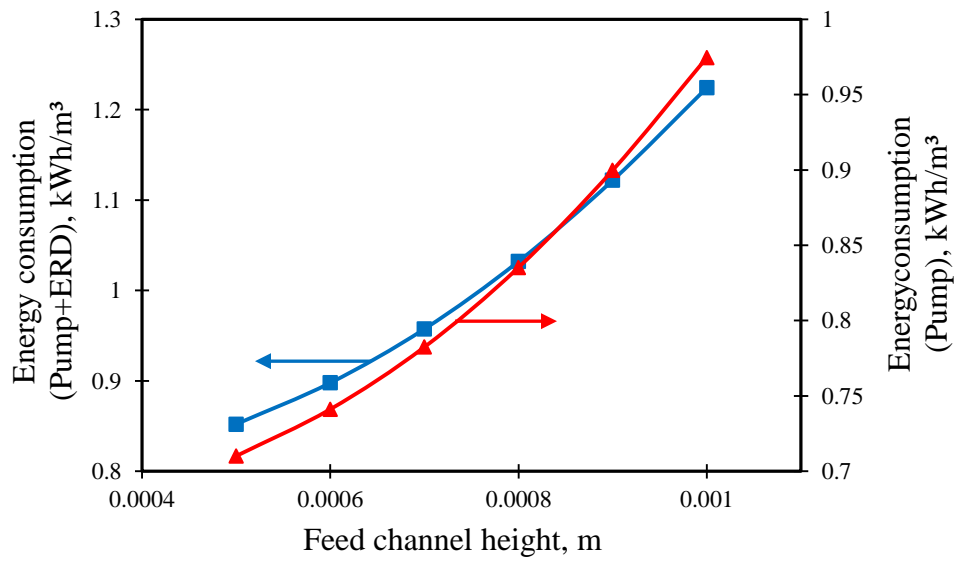


603

604

605

606 **Fig. 5.**



607

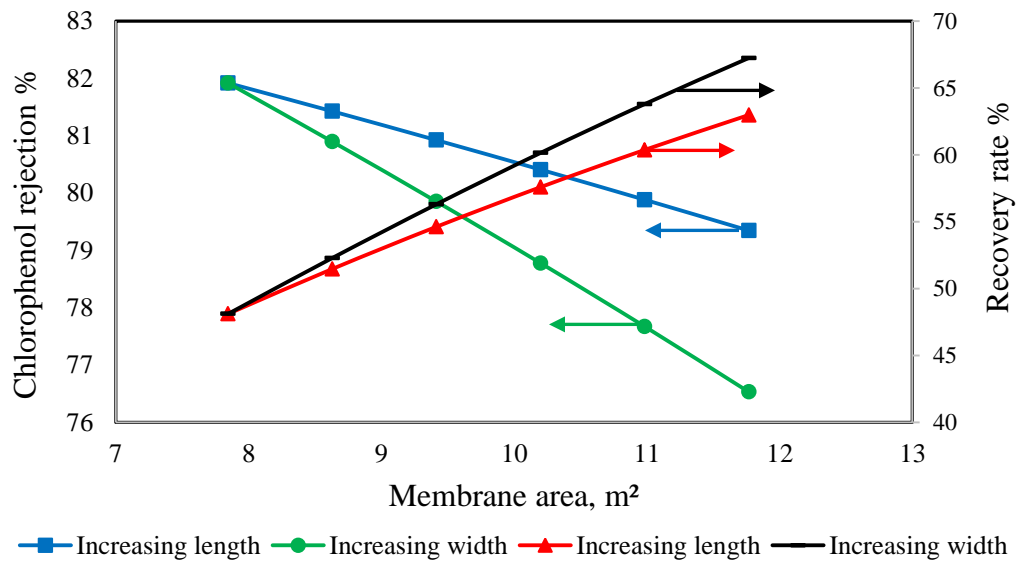
608

609

610

611

612 **Fig. 6.**



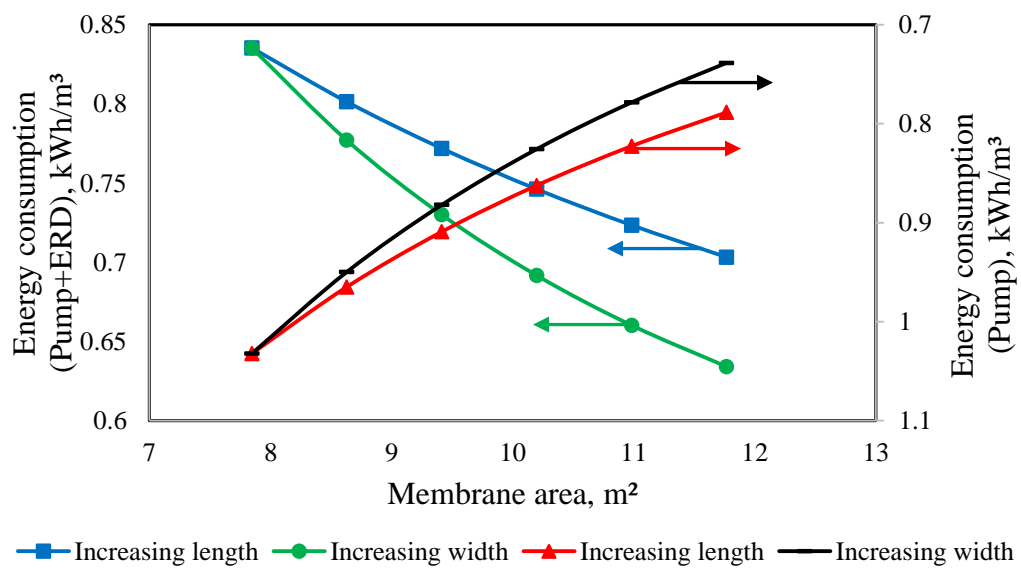
613

614

615

616

617 **Fig. 7.**

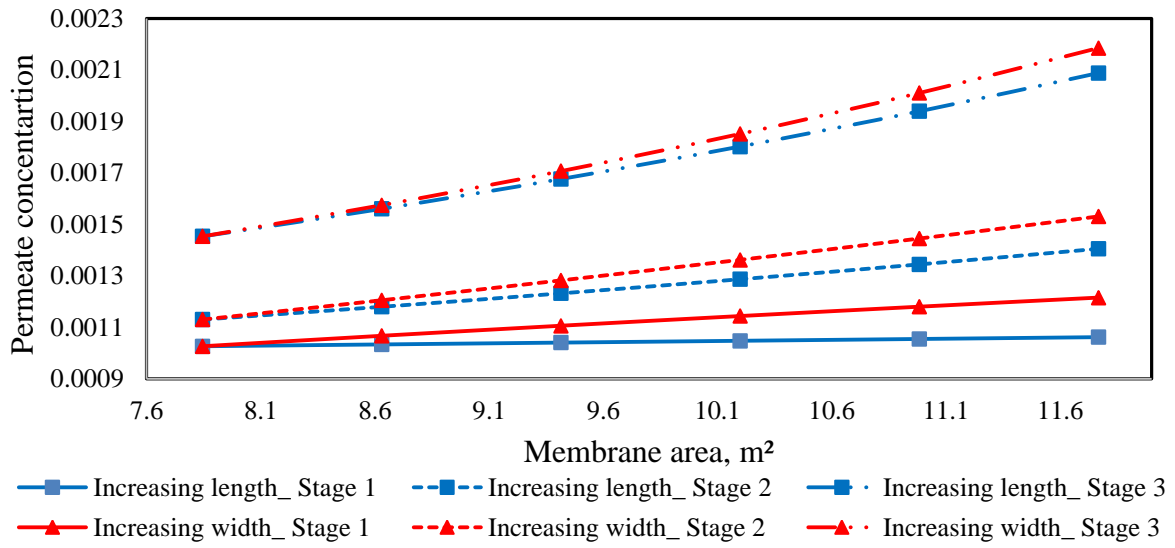


618

619

620

Fig. 8.



621

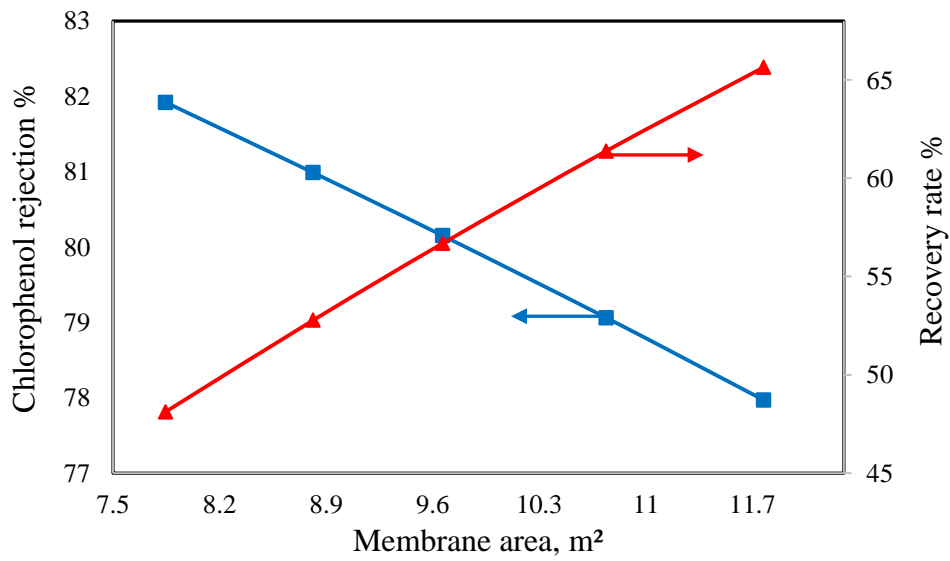
622

623

624

625

Fig. 9.



626

627

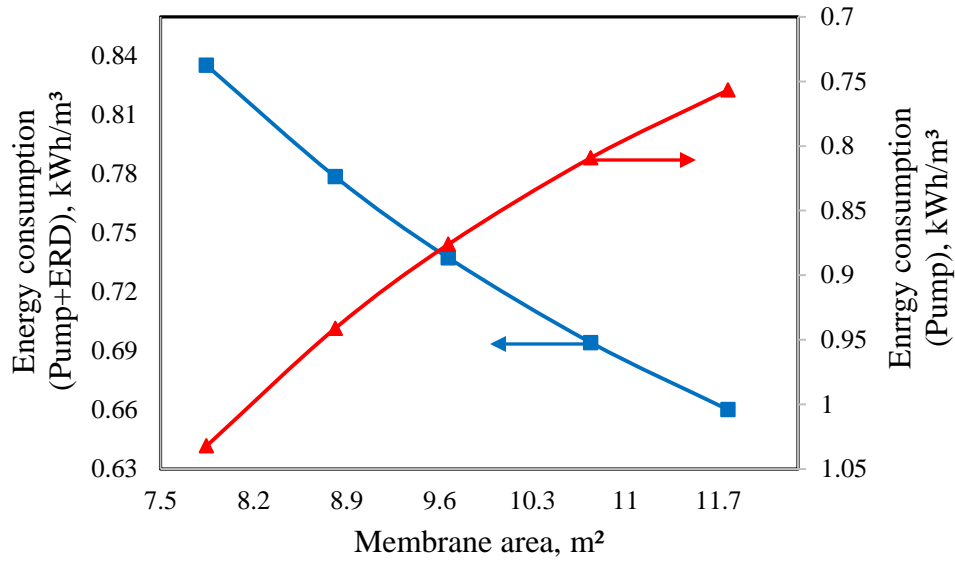
628

629

630

631

Fig. 10.



632
633
634
635
636

Table 1.

Parameter	Value
Membrane material and configuration	TFC aromatic polyamide composite, spiral wound
Model	HM4040-LPE
Feed spacer thickness (t_f)	0.8E-3 m
Permeate channel thickness (t_p)	0.5E-3 m
Number of turns	30
Module length (L)	0.934 m
Module width (W)	8.4 m
Membrane area (A)	7.845 m ²
Membrane volume	6.2764E-3 m ³

637
638
639
640
641

Table 2.

Parameter	Units	Value
A_w	m/atm s	9.5188E-7
B_s	m/s	8.468E-8
b	atm s/m ⁴	8529.45

642
643
644
645
646

647 **Table 3.**

Simulation set	Total energy consumption, kWh/m ³		Chlorophenol rejection% <i>Rej</i> _(Total)	Total water recovery% <i>Rec</i> _(Total)
	<i>T. E. C. 1</i> (Pump)	<i>T. E. C. 2</i> (Pump+ERD)		
1	1.165	0.979	77.039	31.256
2	0.922	0.746	80.803	53.834
3	1.127	0.919	80.281	39.902
4	0.946	0.775	84.632	52.466
Sundaramoorthy <i>et al.</i> ¹³	2.034	---	83.000	22.000

648

649

650

651

652

653 **Table 4.**

Parameter	Upper limit, m	Lower limit, m
Membrane length	1.4	0.5
Membrane width	12.6	8.4
Feed channel height	0.001	0.0005

654

655

656

657

658

659 **Table 5.**

Stage no.	Optimised membrane dimensions, m			Optimised total energy consumption, kWh/m ³		Optimised chlorophenol rejection % <i>Rej</i> _(Total)	Total water recovery % <i>Rec</i> _(Total)
	<i>L</i>	<i>W</i>	<i>t_f</i>	<i>T. E. C. 1</i> (Pump)	<i>T. E. C. 2</i> (Pump+ERD)		
1	1.4	5.603	0.5E-3	0.927	0.807	93.5	53.555
2	1.092	7.184	0.5E-3				
3	1.4	5.603	0.5E-3				

660

661

662

663

664 **Appendix A**

Table A.1. Mathematical modelling of an individual spiral-wound RO system (Al-Obaidi *et al.*,¹²)

Model Equations	Specifications	Eq. no.
$J_w = A_w \left[\left(\frac{P_{f(in)} + P_{f(out)}}{2} - P_p \right) - \left(R (T + 273.15) (C_w - C_p) \right) \right]$	The permeate flux (m/s)	1
$J_s = B_s (C_w - C_p)$	The solute flux (kmol/m ² s)	2
$\frac{(C_w - C_p)}{(C_b - C_p)} = \exp \left(\frac{J_w}{k} \right)$	The wall solute concentration (kmol/m ³)	3
$U_b = \frac{Q_b}{W t_f}$	The bulk feed velocity (m/s)	4
$Q_b = \frac{Q_f + Q_r}{2}$	The bulk feed flow rate (m ³ /s)	5
$C_b = \frac{C_f + C_r}{2}$	The bulk concentration (kmol/m ³)	6
$C_p = \frac{J_s}{J_w + J_s}$	The permeate solute concentration (kmol/m ³)	7
$Q_f = Q_r + Q_p$	The retentate flow rate (m ³ /s)	8
$Q_f C_f = Q_r C_r + Q_p C_p$	The retentate concentration (kmol/m ³)	9
$Q_p = J_w A$	The total permeated flow rate (m ³ /s)	10
$P_{b(out)} = \left\{ P_{b(in)} - \right.$ $(b L Q_f) + \left(b W \theta \left(\frac{L^2}{2} \right) (\Delta P_{b(out)}) \right) - \left[b^2 W \theta \left(\frac{L^3}{6} \right) Q_f \right] -$ $\left. \left[b^2 W \theta \left(\frac{W \theta}{b} \right)^{0.5} \left(\frac{L^3}{6} \right) (\Delta P_{b(out)} - \Delta P_{b(in)}) \right] \right\}$	The retentate pressure. ¹⁷	11
$\theta = \frac{A_w B_s}{B_s + R (T + 273.15) A_w C_p}$	Parameter in Eq. (11)	12
$\Delta P_{b(in)} = P_{b(in)} - P_p$	The pressure difference at the inlet edge (atm)	13
$\Delta P_{b(out)} = P_{b(out)} - P_p$	The pressure difference at the outlet edge (atm)	14
$Rec = \frac{Q_p}{Q_f} \times 100$	The total permeate recovery (dimensionless)	15
$Rej = \frac{C_f - C_p}{C_f} \times 100$	The solute rejection (dimensionless)	16
$T.E.C.1 = \frac{\left((P_{b(in)} \times 10^{1325}) Q_f \right)}{Q_{p(Total)} \varepsilon_{pump} \times 36E5}$	The specific consumption energy of HPP (kWh/m ³) without ERD	17
$T.E.C.2 = \frac{\left((P_{b(in)} \times 10^{1325}) Q_f (HPP) \right) + \left((P_{b(in)} \times 10^{1325}) Q_f (BP) \right) - \left((P_{b(out)} \times 10^{1325}) Q_r \varepsilon_{ERD} \right)}{Q_{p(Total)} \varepsilon_{pump} \times 36E5}$	The specific consumption energy of HPP (kWh/m ³) with ERD	18
$Q_{f(BP)} = Q_r$	Calculates the feed flow rate of Booster pump	19
$\varepsilon_{ERD} = \frac{P_{b(ERD)}}{P_{b(out)}}$	Calculates the pressure of ERD	20

666

667

668

669

670

Table A.2. Thermophysical properties of chlorophenol

Model Equations	Specifications	Eq. no.
$k = \frac{147.4 D_b Re_b^{0.13} Re_p^{0.739} C_m^{0.135}}{2 t_f}$	The mass transfer coefficient (m/s). ¹³	1
$C_m = \frac{C_b}{\rho_w}$	The dimensionless solute concentration (dimensionless)	2
$D_b = 6.725E - 6 \exp \left\{ 0.1546E - (3 C_f \times 18.0125) - \frac{2513}{(T+273.15)} \right\}$	The diffusivity parameter at the feed channel (m ² /s). ¹⁹	3
$D_p = 6.725E - 6 \exp \left\{ 0.1546E - (3 C_p \times 18.0125) - \frac{2513}{(T+273.15)} \right\}$	The diffusivity parameter at the permeate channel (m ² /s)	4
$\mu_b = 1.234E - 6 \exp \left\{ 0.0212E - (3 C_f \times 18.0153) + \frac{1965}{(T+273.15)} \right\}$	The dynamic viscosity (kg/m s) at the feed channel	5
$\mu_p = 1.234E - 6 \exp \left\{ 0.0212E - (3 C_p \times 18.0153) + \frac{1965}{(T+273.15)} \right\}$	The dynamic viscosity (kg/m s) at the permeate channel	6
$\rho_b = 498.4 m_f + \sqrt{[248400 m_f^2 + 752.4 m_f C_f \times 18.01253]}$	The feed density (kg/m ³)	7
$\rho_p = 498.4 m_f + \sqrt{[248400 m_f^2 + 752.4 m_f C_p \times 18.01253]}$	The permeate density (kg/m ³)	8
$m_f = 1.0069 - 2.757E - 4 (T)$	Parameter in Eqs. (7) and (8)	9
$Re_b = \frac{\rho_b de_b Q_b}{t_f W \mu_b}$	The Reynolds number at the feed channel (dimensionless)	10
$Re_p = \frac{\rho_p de_p J_w}{\mu_p}$	The Reynolds number at the permeate channel (dimensionless)	11
$de_b = 2t_f$ $de_p = 2t_p$	The equivalent diameters of the feed and permeate channels (m)	12

672

673

674

675

676

677

678

679

680

681

682

683

684

685

686

687

688

689

690

Table A.3. Model validation results at several operating conditions

No	P _{b(in)}	T	C _f	Q _f	P _{b(out)} (atm)	⊗ ⊠ ⊡	Q _r × 10 ⁴ (m ³ /s)	⊗ ⊠ ⊡	C _p × 10 ³ (kmol/m ³)	%Err or	Rej	⊗ ⊠ ⊡
----	--------------------	---	----------------	----------------	---------------------------	-------	--	-------	---	---------	-----	-------

	(atm)	(°C)	x10 ³ (kmol/ m ³)	x10 ⁴ (m ³ /s)	Exp.	The.		Exp.	The.		Exp.	The.		Exp.	The.	
1	9.71	30	0.778	2.166	8.3	8.16	1.6	1.59	1.63	-2.2	0.366	0.345	5.5	61.4	62.48	-1.7
2	11.64	30	0.778	2.166	10.08	10.14	-0.6	1.5	1.50	0.3	0.363	0.362	0.2	63.8	62.45	2.1
3	13.58	30	0.778	2.166	12.04	12.14	-0.8	1.37	1.37	0.3	0.36	0.381	-6.0	66.2	62.21	6.0
4	7.77	31	6.226	2.166	6.24	6.145	1.5	1.828	1.84	-0.8	1.657	1.353	18.3	76.7	80.87	-5.4
5	9.71	31	6.226	2.166	8.11	8.129	-0.2	1.75	1.73	0.9	1.491	1.301	12.6	79.8	82.54	-3.4
6	11.64	31	6.226	2.166	9.98	10.10	-1.2	1.641	1.62	0.9	1.475	1.289	12.5	81	83.62	-3.2
7	13.58	31	6.226	2.166	11.85	12.08	-1.9	1.575	1.52	3.5	1.457	1.299	10.7	81.9	84.38	-3.0
8	5.83	30	0.778	2.33	4.46	4.043	9.3	1.957	2.06	-5.2	0.375	0.321	14.2	56.2	61.59	-9.5
9	7.77	30	0.778	2.33	6.35	6.038	4.9	1.86	1.93	-3.5	0.373	0.324	13.0	58.1	62.86	-8.2
10	9.71	30	0.778	2.33	8.22	8.031	2.2	1.742	1.79	-2.8	0.372	0.334	10.0	60.3	63.26	-4.9
11	11.64	30	0.778	2.33	10.09	10.01	0.7	1.639	1.66	-1.3	0.37	0.349	5.6	62.4	63.26	-1.3
12	13.58	30	0.778	2.33	11.96	12.00	-0.3	1.542	1.53	0.7	0.367	0.367	0.0	64.5	63.05	2.2
13	5.83	31	6.226	2.33	4.27	4.027	5.6	2.082	2.12	-1.9	1.726	1.46	15.2	74.5	78.15	-4.9
14	7.77	31	2.455	2.33	6.16	6.011	2.4	1.987	2.01	-1.1	1.645	1.321	19.6	76.6	81.15	-5.9
15	9.71	31	2.455	2.33	8.03	7.996	0.4	1.902	1.90	0.2	1.472	1.263	14.1	79.8	82.83	-3.8
16	11.64	31	2.455	2.33	9.9	9.970	-0.7	1.815	1.79	1.5	1.433	1.244	13.1	81.2	83.91	-3.3
17	13.58	31	2.455	2.33	11.77	11.95	-1.5	1.734	1.68	3.1	1.419	1.248	12.0	82.2	84.68	-3.0
18	7.77	31	1.556	2.583	6.17	5.825	5.5	2.148	2.20	-2.3	0.572	0.46	19.5	67.5	73.65	-9.1
19	9.71	31	1.556	2.583	7.79	7.817	-0.3	2.042	2.07	-1.3	0.553	0.46	16.8	69.7	74.83	-7.3
20	11.64	31	1.556	2.583	9.92	9.799	1.2	1.947	1.94	0.2	0.55	0.469	14.7	71.2	75.51	-6.0
21	13.58	31	1.556	2.583	11.79	11.79	-0.0	1.85	1.81	1.9	0.549	0.484	11.8	72.5	75.93	-4.7
22	9.71	31	2.335	2.583	8.03	7.811	2.7	2.08	2.09	-0.3	0.744	0.606	18.5	72.8	77.91	-7.0
23	11.64	31	2.335	2.583	9.84	9.791	0.4	1.97	1.96	0.3	0.733	0.612	16.5	74.2	78.75	-6.1
24	13.58	31	2.335	2.583	11.74	11.78	-0.3	1.868	1.84	1.4	0.726	0.626	13.8	75.7	79.30	-4.7
25	7.77	31	6.226	2.583	6.03	5.805	3.7	2.253	2.26	-0.5	1.549	1.278	17.4	77.8	81.52	-4.7
26	9.71	31	6.226	2.583	7.9	7.790	1.3	2.17	2.15	0.8	1.486	1.212	18.4	79.4	83.23	-4.8
27	11.64	31	6.226	2.583	9.75	9.765	-0.1	2.09	2.04	2.4	1.387	1.186	14.4	81.5	84.33	-3.4
28	13.58	31	6.226	2.583	11.65	11.74	-0.8	2.012	1.93	4.1	1.325	1.182	10.7	83	85.10	-2.5

691

692

693

694

695